Radical reactions in aqueous solution: use of the *aci*-anion of nitromethane as a spin trap

BRUCE C. GILBERT AND RICHARD O. C. NORMAN
Department of Chemistry, University of York, Heslington, York YO1 5DD, U.K.

Received July 15, 1981

BRUCE C. GILBERT and RICHARD O. C. NORMAN. Can. J. Chem. **60**, 1379 (1982).

The type of radical detected by esr when first-formed short-lived radicals are generated by photolytic, radiolytic, or flow techniques in the presence of nitromethane is shown to depend upon the nature and structure of the transient radical and on the pH. Thus electron-donating radicals may react with CH_3NO_2 itself under certain conditions to give rise to $CH_3NO_2^{-\cdot}$ and the alkoxy nitroxides $CH_3N(OR)O\cdot$. At higher pH, a wide variety of radicals (X) react very readily with the *aci*-anion $CH_2{:}NO_2^-$ to give adducts $XCH_2NO_2^{-\cdot}$ (and, from radicals capable of one-electron transfer, $O_2NCH_2CH_2NO_2^{-\cdot}$). Structural characteristics of adducts $XCH_2NO_2^{-\cdot}$ are described and it is shown how radicals which are normally undetectable in fluid solution can be trapped and recognized in this way. Mechanistic pathways diagnosed with this trap (involving, e.g. alkoxyl radicals, aroyloxyl radicals, aromatic carboxylate cation-radicals) are exemplified.

BRUCE C. GILBERT et RICHARD O. C. NORMAN. Can. J. Chem. **60**, 1379 (1982).

Lorsqu'on produit des radicaux par écoulement, par radiolyse ou par photolyse en présence de nitrométhane, le type de radical détecté par rpe, lorsqu'apparaissent les premiers radicaux de courte vie, dépend de la nature et de la structure du radical intermédiaire et du pH. Ainsi les radicaux électrodonneurs peuvent réagir avec le CH_3NO_2 lui-même dans certaines conditions pour donner le CH_3NO_2 et les alkoxynitroxydes du type $CH_3N(OR)O$. A des pH plus élevés, une grande variété de radicaux (X) réagit très facilement avec l'anion *aci* $CH_2{:}NO_2^{-\cdot}$ en donnant des adduits $XCH_2NO_2^{-\cdot}$ (et le radical $O_2NCH_2CH_2NO_2^{-\cdot}$ à partir des radicaux pouvant subir un transfert d'un électron). On décrit les caractéristiques structurales des adduits $XCH_2NO_2^{-\cdot}$ et on montre comment les radicaux non détectables normalement en solution fluide peuvent être piégés et identifiés de cette façon. On propose un mécanisme relatif à ce piégeage (qui fait intervenir par exemple les radicaux alkoxy, les radicaux aryloxy et les radicaux cationiques du type carboxylate aromatique) et on l'illustre par des exemples.

[Traduit par le journal]

Introduction

The increase in our understanding of the radical chemistry of nitro compounds has largely gone hand-in-hand with the development of esr spectroscopy as a physical–organic tool for probing the structures and mechanisms of reaction of free radicals.

Thus both electrochemical techniques, with aromatic (1) and aliphatic (2) substrates, and alkali-metal reduction (3) methods were developed to study relatively stable nitro radical-anions; mechanistic information often resulted, as in the reductive dehalogenation of some aromatic examples (4), electron-transfer reactions involving carbanions and *p*-nitrobenzyl halides (5), and the formation of nitroxides during alkali-metal reduction of nitroalkanes (6). Nitro compounds also provided early examples of the correlation of esr parameters with the results of molecular orbital calculations (1*b*), the occurrence of restricted rotation (for *p*-nitrobenzaldehyde$^{-\cdot}$ (1*a*)), steric inhibition of resonance when bulky substituents are present in the *ortho* positions (1*b*), buttressing effects (7), and many instances of alternating line-width phenomena (8) and solvent effects (2, 9). More recent examples include investigations of substituent effects for $ArNO_2^{-\cdot}$ (10) (and a correlation between angles of twist and rates of electron-transfer from $\cdot CMe_2OH$), pK_a values and hydrogen-bonding effects in aromatic radical-anions (11) and more sophisticated MO calculations (12).

A further important area, to be described here, is the use of esr to study the reactions of nitroalkanes in the presence of short-lived radicals in aqueous solution, and, in particular, the development of "spin-trapping" methods employing both CH_3NO_2 and its *aci*-anion $CH_2{:}NO_2^-$.

Experimental method

Most of the reactions to be described have been studied using an esr spectrometer in conjunction with simple two- or three-way flow systems in which separate solutions are mixed ca. 70 ms before passage of the combined solution through the cavity of the spectrometer; although in the earlier experiments gravity feed was normally employed, it is customary now to maintain the flow with a peristaltic pump. Full experimental details of the flow systems, spectrometers, measurement and calibration of spectra, reagent concentrations, and control and measurement of pH have been given previously (ref. 13 and references therein) and will not be repeated here.

Results and discussion

Radical reactions of nitromethane in aqueous solution

A variety of redox reactions, normally employing titanium(III) as reductant, have been utilized to generate "primary" radicals (see, e.g. reactions [1]–[4] (13, 14)) whose further reactions have been studied. It should be noted that when a reactive first-formed radical (e.g. $\cdot OH$) is scavenged in the

0008-4042/82/121379-13$01.00/0

flow system by reaction solely with an excess of an added substrate (RH), then if the resulting radical R· is short-lived (i.e. $2k_t$ ca. 10^9 dm^3 mol^{-1} s^{-1}), a pseudo-steady state condition for the formation and destruction of R· is achieved and kinetic analysis of the reaction system is possible (15); applications will be described later. We shall also describe results, analogous to those obtained using flow systems, from investigations in which ·OH is generated by *in situ* radiolysis (16).

[1] $Ti^{III} + H_2O_2 \rightarrow Ti^{IV} + \cdot OH + OH^-$

[2] $Ti^{III} + S_2O_8^{2-} \rightarrow Ti^{IV} + SO_4^{-\cdot} + SO_4^{2-}$

[3] $Ti^{III} + NH_3OH^+ \rightarrow Ti^{IV} + NH_3^{+\cdot} + OH^-$

[4] $Ti^{III} + RO_2H \rightarrow Ti^{IV} + RO\cdot + OH^-$

(*a*) *Electron transfer and addition to* CH_3NO_2. When ·OH is generated in the presence of ethanol (0.6 mol dm^{-3}) and nitromethane (0.03 mol dm^{-3}) at pH ca. 8, the strong esr signal detected has a(N) 2.57, a(3H) 1.20 mT, with g 2.0051 (17); this is assigned to the nitromethane radical-anion $MeNO_2^{-\cdot}$ (**1**), whose structure will be described later. This radical also results under similar circumstances in the presence of other alcohols with an α-hydrogen atom, and it is concluded that the α-hydroxyalkyl radicals formed by reaction of the electrophilic hydroxyl radical with added alcohols react via an overall one-electron transfer reaction (facilitated by the +M effect of the oxygen substituent). In contrast, a variety of different radicals with parameters somewhat similar to this is detected from the reactions of the same alcohols at low pH (ca. 2) and from the corresponding ether-derived species at both pH 2 and 8. For example, the radical formed from ·CHMeOH and $MeNO_2$ at pH 2 has a(N) 2.79, a(3H) 1.02 mT, g 2.0052; that from ·CHMeOEt and $MeNO_2$ (at both pH 2 and 8) has a(N) 2.74, a(3H) 0.86 mT, with g 2.0052. These signals are assigned to the alkoxynitroxide radical-adducts $CH_3N(O\cdot)OCHMeOH$ (**2**) and $CH_3N(O\cdot)OCHMeOEt$ (**3**), formed in reactions which are again facilitated by the +M effect of the oxygen substituents as indicated in Scheme 1 (for an alcohol-derived radical) and Scheme 2 (for an ether-derived example); in the former the base-catalysed route to the radical-anion is also indicated. The reactions of other aliphatic nitrocompounds, the formation of aromatic analogues of the adducts (with splittings from protons in the alkoxy moiety), and the production of nitroxides from RNO_2H (formed in acid solution) have also been described (17). It should be stressed that reactions as shown in Schemes 1 and 2 are typical of radicals with a *reducing* capacity, and are not shown by, for example, Me· (see below).

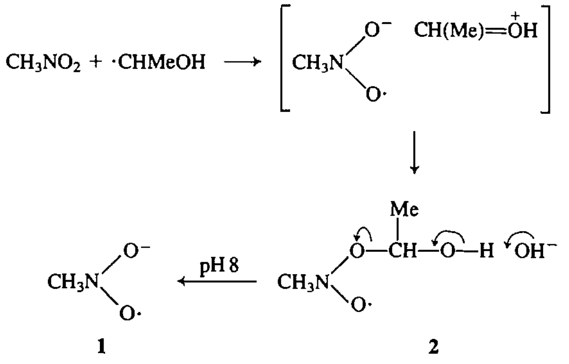

	1		2
a(N)	2.57 mT	a(N)	2.79
a(3H)	1.20 mT	a(3H)	1.02 mT
g	2.0051	g	2.0052

SCHEME 1

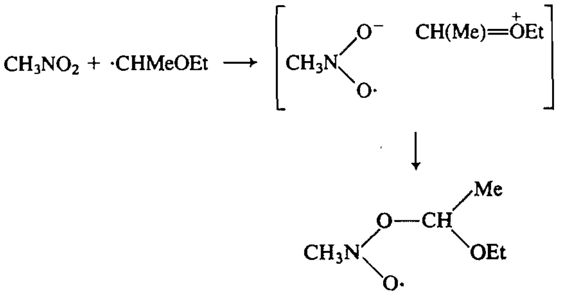

	3
a(N)	2.74 mT
a(3H)	0.86 mT
g	2.0052

SCHEME 2

(*b*) *Reactions of* $CH_2{:}NO_2^-$*: addition and oxidative electron-transfer*. The attractions of $MeNO_2$ as a spin-probe for radicals in aqueous solution include not only its ready availability and its solubility in water but also the relative stability of its *aci*-anion $CH_2{:}NO_2^-$ (CH_3NO_2 has pK_a 10.2 (18)); at pH values ≥ ca. 8.5 (which can be readily achieved in flow system experiments) a significant — and adjustable — concentration of the *aci*-anion can be achieved and its high reactivity exploited.

For example, when ·OH is generated either by the redox reaction [1] in a flow system (19) or by *in situ* γ-irradiation (16) in the presence of N_2O (to convert e$^-$ into ·OH), its resultant reaction with $CH_2{:}NO_2^-$ leads to the detection of the adduct (**4**), with a(N) 2.49, a(2H) 0.89 mT, g 2.0051 (reaction [5]). Several points are important here; firstly, the very rapid rate of *trapping* of ·OH is notable (k_5 has been estimated as 9 × 10^9 dm^3 mol^{-1} s^{-1} from a pulse radiolysis study (20); in contrast, the electrophilic ·OH radical is relatively unreactive towards CH_3NO_2 (21)); secondly, the fact that whereas ·OH itself is undetectable in fluid solution (22), strong signals from the adduct (**4**) are readily obtained (it has been shown (21) that the related radical-ion $CH_3NO_2^{-\cdot}$, and to a less marked extent $CH_3N(O\cdot)OH$, are significantly longer-lived than simple short-lived organic radicals in solution); and thirdly, that the parameters for the radical detected characterize its structure (see later).

$$[5]\quad HO\cdot + CH_2{:}NO_2^- \xrightarrow{k_5} \underset{\mathbf{4}}{HOCH_2NO_2^{-\cdot}}$$

Reaction of ·OH with dimethyl sulphoxide in the presence of $CH_2{:}NO_2^-$ leads to the formation and trapping of Me· (reactions [6] and [7]) to give the easily recognized esr signal of the nitro*ethane* radical-anion (**5**) (Fig. 1) (23, 24); this spectrum (with *a*(N) 2.60, *a*(2H) 0.97, *a*(3H) 0.05 mT, *g* 2.0050) illustrates the narrow line-widths (and hence good resolution) obtained with this type of trap, which, as in this case, often reveals the presence of a characteristic γ-proton coupling. From the point of view of structural verification it is helpful that independent routes to the spin-adducts are often available (e.g. in this case, the electron-transfer reaction of ·CHMeOH and nitroethane at pH ca. 8; *cf*. Scheme 1). We might also note here that relatively electron-rich radicals, e.g. ·CHMeOH, can also be trapped (24) via addition to $CH_2{:}NO_2^-$ at pH ca. 9 (reaction [8]); the parameters of **6**, and the general usefulness of this spin-trapping reaction, will be discussed subsequently.

$$[6]\quad HO\cdot + Me_2S{=}O \rightarrow Me\cdot + MeSO_2H$$

$$[7]\quad Me\cdot + CH_2{:}NO_2^- \rightarrow \underset{\mathbf{5}}{MeCH_2NO_2^{-\cdot}}$$

$$[8]\quad \cdot CHMeOH + CH_2{:}NO_2^- \rightarrow \underset{\mathbf{6}}{HOCHMeCH_2NO_2^{-\cdot}}$$

The spectrum detected (25) during the oxidation of nitromethane in a flow system at pH ca. 9 with $SO_4^{-\cdot}$ is identical to that observed (26) in the one-electron reduction of 1,2-dinitroethane with $\cdot CO_2^-$ and is accordingly assigned to the radical-anion (**7**) (with *a*(N) 2.54, *a*(2H) 1.12, *a*(2H) 0.04 mT, *g* 2.0050); evidently the sulphate radical-anion effects overall one-electron oxidation of the *aci*-anion to $\cdot CH_2NO_2$, which is subsequently trapped (reactions [9] and [10]). The spectrum of the *adduct* $^-O_3SOCH_2NO_2^{-\cdot}$ is also detected as a minor component in both flow and photolytic experiments. The oxidative reaction sequence illustrated in reactions [9] and [10] is also brought about by the anion-radical $Br_2^{-\cdot}$ (from Br^- and ·OH) and some related species (16).

$$[9]\quad CH_2{:}NO_2^- + SO_4^{-\cdot} \rightarrow \cdot CH_2NO_2 + SO_4^{2-}$$

$$[10]\quad \cdot CH_2NO_2 + CH_2{:}NO_2^- \rightarrow \underset{\mathbf{7}}{O_2NCH_2CH_2NO_2^{-\cdot}}$$

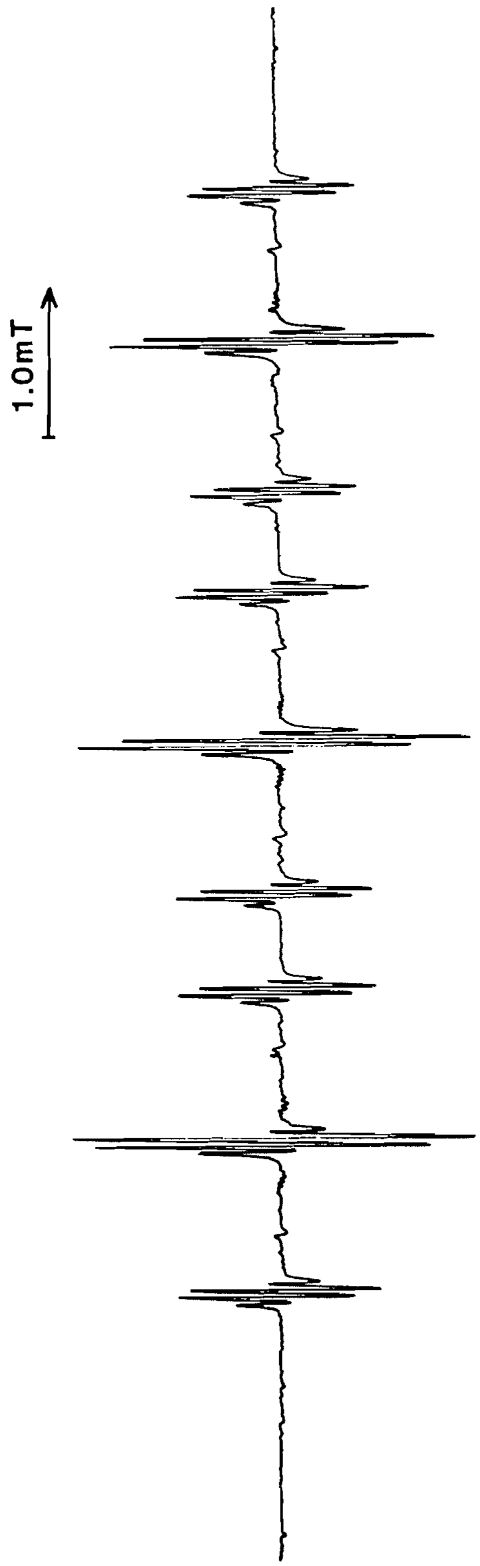

FIG. 1. Electron spin resonance spectrum of $MeCH_2NO_2^{-\cdot}$, formed from the reaction of Me· (from ·OH and Me_2SO) and $CH_2{:}NO_2^-$ at pH ca. 9.

(c) Hydrogen-atom abstraction from CH_3NO_2. Evidence has been adduced that the radical $\cdot CH_2NO_2$ is also obtained by reaction of the parent nitroalkane with ·Me under appropriate conditions (23). This follows from the detection in the Ti^{III}–H_2O_2–Me_2SO–$MeNO_2$ system of, at pH ca. 6, the radical-anion $EtNO_2^{-\cdot}$ and, at pH ca. 2, the conjugate acid EtN(O·)OH (with a(N) 2.81, a(2H) 0.91, a(1H) 0.32 (23), g 2.0049 (26)): under these conditions the concentration of $CH_2{:}NO_2^-$ formed by ionization of nitromethane is too low (even at pH 6) to serve effectively as a trap and another route to its generation is required. It is proposed that both $CH_2{:}NO_2^-$ and, at lower pH, the conjugate acid $CH_2{:}NO_2H$ are formed by one-electron reduction by Ti^{III} of $\cdot CH_2NO_2$ generated in the initial hydrogen-abstraction reaction (see Scheme 3) and that they can then serve as effective spin traps. It is suggested that k_{11} is ca. 10^3 dm^3 mol^{-1} s^{-1} under these conditions and that both trapping reactions [7] and [13] are very rapid. Electron spin resonance experiments of this sort also enable pK_a to be determined for the nitro radical-anion protonation equilibria (e.g. a value for pK_a of 4.4 was obtained (23) for $Pr^iNO_2H \rightleftharpoons Pr^iNO_2^{-\cdot} + H^+$, these radicals being generated from Me· and $CHMe{:}NO_2H$ and $CHMe{:}NO_2^-$ in experiments with nitroethane). A broadly similar mechanism, involving loss of bromide ion from a first-formed radical-anion and subsequent reduction of the α-nitro radical is thought to explain the formation of $O_2NCH_2CH_2NO_2^{-\cdot}$ in the reaction of Ti^{III} with $BrCH_2NO_2$ (see Scheme 4) (28).

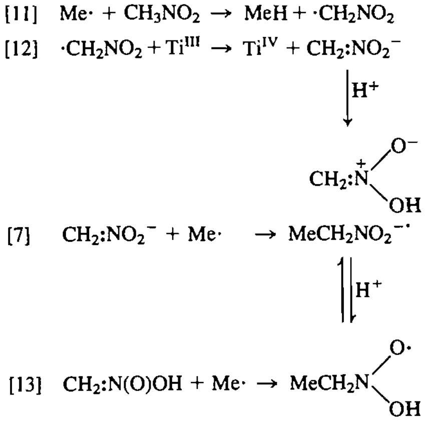
[11] $Me\cdot + CH_3NO_2 \rightarrow MeH + \cdot CH_2NO_2$

[12] $\cdot CH_2NO_2 + Ti^{III} \rightarrow Ti^{IV} + CH_2{:}NO_2^-$

[7] $CH_2{:}NO_2^- + Me\cdot \rightarrow MeCH_2NO_2^{-\cdot}$

[13] $CH_2{:}N(O)OH + Me\cdot \rightarrow MeCH_2N(O\cdot)OH$

SCHEME 3

$$\begin{aligned}
BrCH_2NO_2 + Ti^{III} &\rightarrow Ti^{IV} + BrCH_2NO_2^{-\cdot}\\
BrCH_2NO_2^{-\cdot} &\rightarrow Br^- + \cdot CH_2NO_2\\
\cdot CH_2NO_2 + Ti^{III} &\rightarrow Ti^{IV} + CH_2{:}NO_2^-\\
\cdot CH_2NO_2 + CH_2{:}NO_2^- &\rightarrow O_2NCH_2CH_2NO_2^{-\cdot}
\end{aligned}$$

SCHEME 4

Structural properties of $XCH_2NO_2^{-\cdot}$

In assessing the usefulness of the *aci*-anion $CH_2{:}NO_2^-$ as a spin trap it is helpful to discuss briefly what is known about the structures of the radical-anions $RCH_2NO_2^{-\cdot}$ and to examine the sensitivity of the esr parameters (a(N), a(β-H), long-range couplings, line-widths, and g-values) to variations in the nature of the addend X.

It has been suggested (12*a*) that the enhanced nitrogen splitting of ca. 2.5 mT observed for aliphatic nitro radical-anions and the corresponding alkoxynitroxides, in comparison with typical values of a(N) of ca. 1.5 mT for dialkyl nitroxides, is a result of the non-planarity of the bonds at the radical centre; in contrast, most nitroxides are deduced to be essentially planar at the nitrogen atom (29). This conclusion is supported by the results (12*a*) from INDO calculations on $MeNO_2^{-\cdot}$ and $EtNO_2^{-\cdot}$ (for which an angle for out-of-plane bending at the N—O bonds of ca. 6° is suggested) and by the estimate from anisotropic spectra of a $2p{:}2s$ ratio of ca. 11.5 for the orbital of the unpaired electron in nitroalkane radical-anions and related alkoxynitroxides (30). Despite the lack of planarity at the radical centre, it nevertheless appears (12*a*) that the angular dependence of the β-proton splitting in $RNO_2^{-\cdot}$ (R = Me, Et) essentially follows the $B\cos^2\theta$-type expected for hyperconjugative interaction in planar π-radicals (for $MeNO_2^{-\cdot}$ the calculated (INDO) variation of a(β-H) with θ is

$$a(\beta\text{-H}) = 0.023 + 0.359\cos\theta + 2.114\cos^2\theta \text{ mT}$$

i.e. with the last term dominant). Variations in a(N) and $a(CH_2)$ with structure can generally be interpreted in terms of alterations to the geometry of the radical centre as well as to conformational changes, as will subsequently be explained.

(a) Carbon-centred radicals. Table 1 contains details of the esr parameters of some nitro radical-anions formed by trapping carbon-centred radicals (generated in a variety of reactions) with $CH_2{:}NO_2^-$ (24). Although most of these can actually be directly detected under certain circumstances, several others (e.g. Ph·, ·COMe) are generally undetectable by esr under these conditions.

Radicals of the type $RCH_2NO_2^{-\cdot}$ are normally characterized by a nitrogen splitting in the range 2.53–2.60 mT and a β-proton triplet splitting of ca. 1.0 mT; in addition, long-range coupling to γ-CH_2 protons and, sometimes, to δ-protons can be observed. This provided crucial diagnostic evidence for the formation of certain radicals, e.g. $\cdot CH_2CHO$ in the base-catalysed rearrangement of $\cdot CH(OH)CH_2OH$ from glycol.

Two other trends are noticeable, and their recognition assists radical diagnosis and hence mech-

TABLE 1. Electron spin resonance parameters for adducts $RCH_2NO_2^{-\cdot}$ formed from carbon-centred radicals[a,b]

Radical	Reaction employed	Hyperfine splitting/mT		
		a(N)	*a*(CH_2)	*a*(γ,δ-H)
Me·	HO·/Me_2SO HO·/$MeCHO/H_2O_2$	2.60	0.97	0.05 (3H)
Et·	$SO_4^{-\cdot}/EtCO_2^-$	2.54	1.01	0.06 (2H) 0.03 (3H)
·CH_2OH	·OH/MeOH	2.55	1.07	0.04 (2H)
·$CH_2CO_2^-$	·OH/$MeCO_2^-$	2.60	1.00	0.07 (2H)
·$CH_2CH_2CO_2^-$	·OH/$EtCO_2^-$ $SO_4^{-\cdot}/^-O_2CCH_2CH_2CO_2^-$	2.55	1.02	0.06 (2H)
·CH_2COCH_3	·OH/$Me_2C{=}O$	2.60	1.07	0.06 (2H)
·CH_2CHO	·OH/$HOCH_2CH_2OH,OH^-$	2.60	1.05	0.06 (2H) 0.05 (1H)
·CMe_2OH	·OH/Me_2CHOH	2.43[c]	1.01[c]	
·CMe_3	HO·/HC(O)OBu^t $SO_4^{-\cdot}/Me_3CCO_2^-$	2.37	0.87	
Ph·	$SO_4^{-\cdot}/PhCO_2^-$	2.59	0.95	
·COMe	HO·/MeCHO	2.43	0.77	
·CO_2Et	HO·/HCO_2Et	2.50	0.78	
·CCl_3	HO·/CCl_4, $CHCl_3$	2.21[d]	0.77[d]	

[a] Data taken from ref. 24.
[b] $g = 2.0050$ except where stated otherwise.
[c] Line broadening: see text.
[d] $g = 2.0052$.

anistic deductions (though mechanistic features will not be elaborated here). The first is the small but significant decrease in *a*(N) associated with bulky β-substituents (cf. in particular, values of *a*(N) of 2.37 and 2.21 mT for adducts with ·Bu^t and ·CCl_3 respectively (the enhanced *g*-value for the latter is also notable)); this we attribute to a tendency towards *flattening* of the pyramidal nitro-group induced by the increased size of R. The second is the reduction in *a*(β-H) for such substituents (cf. 0.77 mT for R = CCl_3); this we attribute to increased conformational preference for the eclipsed structures **8***a* and **8***b*. The line-width alternation of the 1:2:1 pattern from the β-protons in, e.g. $HOCMe_2CH_2NO_2^{-\cdot}$, and related radicals (25), presumably reflects restricted rotation about either the C—N or the C_β—C_γ bonds or both.

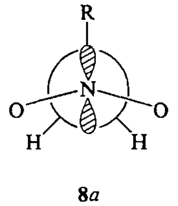

8*a*

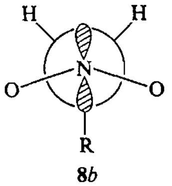

8*b*

(*b*) *Spin-adducts from oxygen-centred and nitrogen-centred radicals.* Table 2 contains details of spin-adducts formed from $CH_2{:}NO_2^-$ and some short-lived oxygen- and nitrogen-centred radicals in aqueous solution. The adducts of the oxygen-centred radicals (which themselves are not directly detectable in aqueous solution) are characterized by rather low *a*(N) and *a*(β-H) values (see above) which suggests that the β C—O bond tends to eclipse the orbital of the unpaired electon (and probably lowers *a*(N) by favouring (flattened) structures of type **9**; cf. ·$CH(OH)CH_2OH$ and other radicals with an inductively electron-withdrawing β-substituent and a +M substituent at the radical centre (34)). Further evidence for some assignments derives from changes in the relative concentrations of different adducts with the concentration of the trap; for example, in the oxidation (32) of benzoate with $SO_4^{-\cdot}$ the assignments of adducts **10** (see Table 2) and **11** (see Table 1) are consistent with the increase in concentration of the former, with respect to the latter, as [$CH_2{:}NO_2^-$] is increased so that addition of $PhCO_2$· to trap competes more effectively with fragmentation (see e.g. Fig. 2). Kinetic applications of this type of study will be described later, but it may be noted that simple acyloxy radicals (RCO_2·) fragment too rapidly for trapping in this way (35).

The formation of amino radicals and alkylamino radicals in the one-electron reduction (33) of hydroxylamine and *N*-alkylhydroxylamines, respectively, is confirmed by the detection of spin-adducts with $CH_2{:}NO_2^-$ (see Table 2); these possess β-nitrogen couplings as well as long-range splittings from N—H and *N*-alkyl protons. The first-formed radicals in these systems (e.g. ·NHMe) are not detected directly under our conditions, evidently due to the occurrence of very rapid reactions including rearrangement (to α-amino-

TABLE 2. Electron spin resonance spectra of spin adducts $RCH_2NO_2^{-\cdot}$ formed from oxygen- and nitrogen-centred radicals

		Hyperfine splitting/mT			
Radical	Method of generation	*a*(N)	*a*(2H)	*a*(other)	*g*
·OH	Ti^{III}/H_2O_2[a]	2.45	0.89		2.0051
	e^-/H_2O[b]	2.523	0.904		2.00502
·OPr	Ti^{III}/PrOOH[c]	2.38	0.85		2.0050
·OPr^i	Ti^{III}/Pr^iOOH[d]	2.39	0.85		2.0050
$PhCO_2$·	$SO_4^{-\cdot}/PhCO_2^-$[e]	2.40	0.74		2.0050
·NH_2	Ti^{III}/NH_2OH[a]	2.55	0.89	0.11 (1N) 0.05 (2H)	2.0051
·NHMe	Ti^{III}/NHMeOH[f]	2.48	0.915	0.15 (N) 0.02 (NH) 0.01 (NMe)	2.0051
·N_3	·OH/N_3^-[b]	2.474	0.546	0.273 (γ-N) 0.027 (2N)	2.00513

[a] Reference 19.
[b] Reference 16.
[c] Reference 14.
[d] Reference 31.
[e] Reference 32.
[f] Reference 33.

alkyl radicals), hydrogen abstraction from parent hydroxylamine, and, possibly, one-electron reduction. Trapping of the azido radical N_3· (from azide ion and ·OH, generated radiolytically) leads to the formation of an adduct with long-range coupling from all the nitrogen atoms (see Table 2) (16); a structure with a linear arrangement of the azido nitrogen atoms, $\bar{N}{=}\overset{+}{N}{=}NCH_2NO_2^{-\cdot}$ is preferred.

(*c*) *The trapping of sulphur- and phosphorus-centred radicals*. Table 3 illustrates the potential of this spin-trapping method in characterizing a variety of first-formed radicals, and hence in providing useful mechanistic information, in both radiolysis (16) and flow (36–40) studies. This is nowhere more important than in probing the mechanisms of oxidation of sulphur-containing compounds, especially as most sulphur-centred radicals (e.g. thiyl radicals, RS·) are not directly detectable yet play a key rôle in oxidation pathways. The most notable features of these trapped adducts are the particularly low nitrogen and β-proton splittings, which indicate that there is strong preference for the eclipsed conformation (**12**) (cf. also radicals of the type ·CH_2CH_2SR (41)), as well as, in most cases, enhanced *g*-values suggestive of spin-transfer from the radical centre. Recognition of these features leads to the proposal for **13** as the structure of the adduct formed from the reaction of ·OH with $S_2O_3^{2-}$ in the presence of $CH_2{:}NO_2^-$ (16, 36). Further useful information comes from long-range coupling "across sulphur" in the adducts with ·SCN (**14**), $(Pr^iO)_2P(S)S$· (**15**) (the parent radical's esr spectrum can be detected (42) in fluid media at low temperature but the line-width increases with temperature to render it undetectable under ambient conditions), and in thioalkyl adducts $RCH_2SCH_2NO_2^{-\cdot}$ (**16**) (see Fig. 3). Phosphorus-centred radicals are trapped to give species with large (3–4 mT) β-phosphorus splittings, and, in one case, detectable interaction with a P—H proton (**17**).

(*d*) *Magnetic inequivalence due to chirality*. A further aid to correct structural identification of adducts is the recognition that for radicals $XYZCCH_2NO_2^{-\cdot}$ in which three different groups are

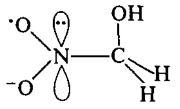

9

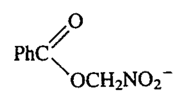

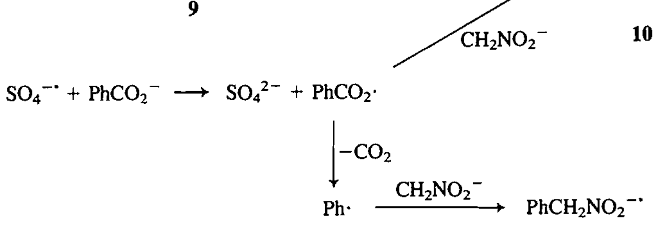

10

11

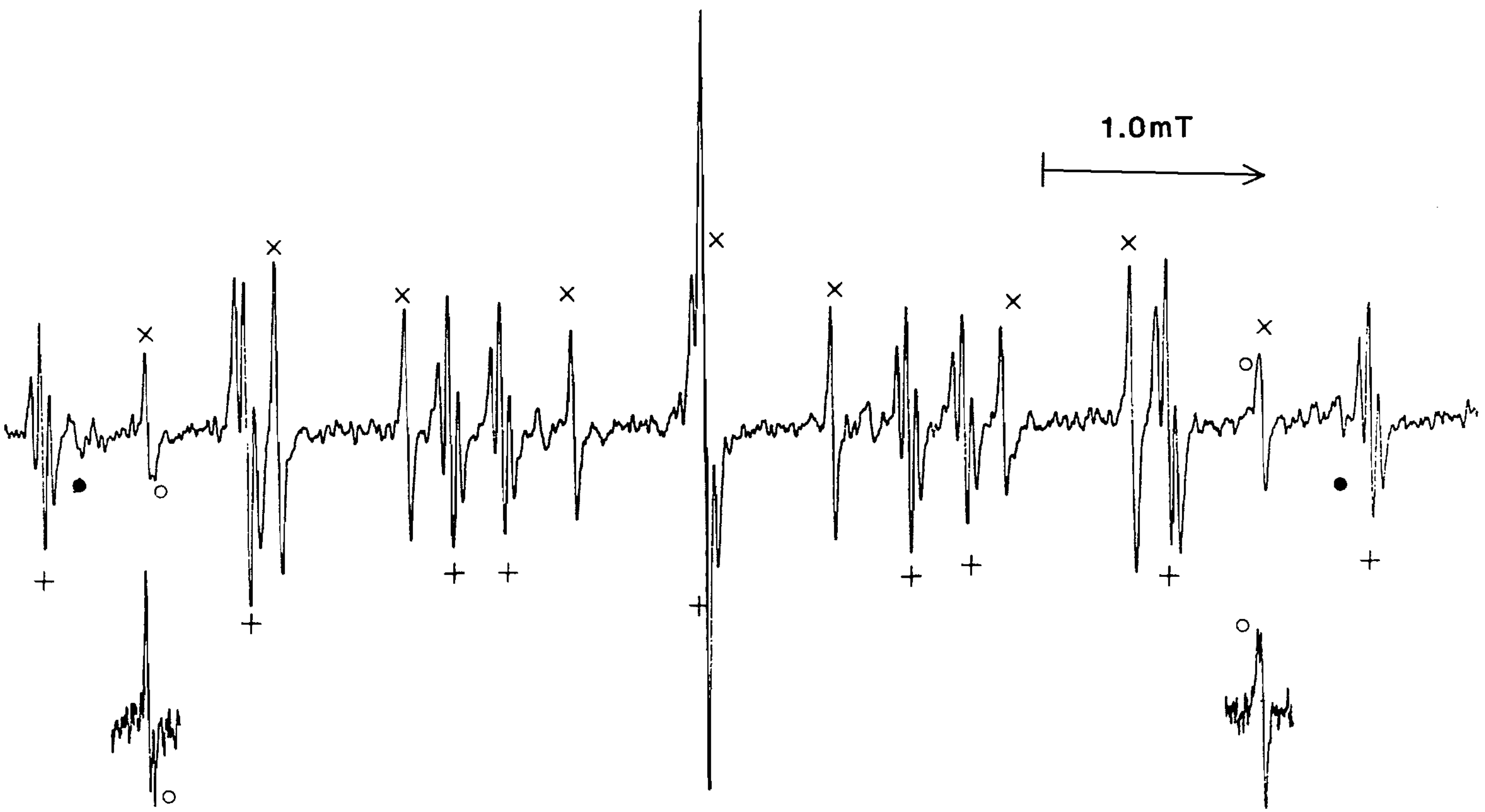

FIG. 2. Electron spin resonance spectra of radical-anions detected during the reaction of $SO_4^{-\bullet}$ and $ArCO_2^-$ (Ar = 3-chlorophenyl) in the presence of a relatively high concentration of $CH_2NO_2^-$ (0.015 mol dm^{-3}). The most intense signals are from $O_2NCH_2CH_2NO_2^{-\bullet}$ (+) and $ArCO_2CH_2NO_2^{-\bullet}$ (×); traces of signals from $^-O_3SOCH_2NO_2^{-\bullet}$ (○) and $ArCH_2NO_2^{-\bullet}$ (●) may also be discerned.

TABLE 3. Electron spin resonance spectra of spin-adducts $RCH_2NO_2^{-\cdot}$ formed from sulphur- and phosphorus-centred radicals

		Hyperfine splitting/mT				
Substrate (reaction with ·OH)	Radical	a(N)	a(β-H)	a(other)	g	Footnote
S^{2-}	$\cdot S^-$	2.436	0.664		2.00584	a,b
SO_3^{2-}	$\cdot SO_3^-$	2.219	0.750		2.00498	a,b
$S_2O_3^{2-}$	$\cdot S_2O_3^-$	2.394	0.600		2.00551	a,b
SCN^-	·SCN	2.169	0.339	0.031(N)	2.00616	a
$S(CH_2CMe_2OH)_2$	$\cdot SCH_2CMe_2OH$	2.42	0.580	0.080(2H)	2.0056	c
$(Pr^iO)_2P(S)S^-$	$\cdot S(S)P(OPr^i)_2$	2.325	0.538	0.100(P)	2.0055	d
HPO_3^{2-}	$\cdot PO_3^{2-}$	2.49	1.07	3.14(P)	2.0050	e,f
$H_2PO_2^-$	$HPO_2^{-\cdot}$	2.51	1.01	2.92(P) 0.15(P—H)	2.0050	e,f
$PhP(H)O_2^-$	$PhPO_2^{-\cdot}$	2.45	1.01	3.34(P)	2.0050	
$(EtO)_2P(O)H$	$(EtO)_2P(O)\cdot$	2.470	0.980	3.773(P)	2.0050	d

[a] Data from ref. 16; ·OH generated photolytically.
[b] See also ref. 34.
[c] Reference 37.
[d] Reference 38.
[e] Reference 39.
[f] See also refs. 16, 40.

FIG. 3. Electron spin resonance spectrum of the adduct (16) of $\cdot SCH_2CH_2OH$ (from ·OH and 2-mercaptoethanol) and $CH_2NO_2^-$.

attached to the γ-carbon, the adjacent methylene protons are rendered non-equivalent (diastereotopic) by the chirality at C_γ, and two non-equivalent splittings result (with consequently a 1:1:1:1 pattern for the β-protons). Examples are given in Table 4 and in Figs. 4 and 5. It should be stressed that this phenomenon occurs *even in the absence of restricted rotation*; where restricted rotation also occurs the inner two lines of the β-protons' 1:1:1:1 pattern are broadened compared with the outer lines (see e.g. the spectrum of $^-O_2CCH_2CH(CO_2^-)CH_2NO_2^{-\cdot}$ in Fig. 4); the crucial observation in this and related examples is that, as the temperature is raised, the inner two lines simply sharpen but do not coalesce, as would have been expected had restricted rotation alone been the cause of inequivalence.

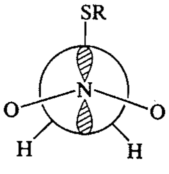

12

$^-O_3S—SCH_2NO_2^{-\cdot}$

13

$NCS—CH_2—NO_2^{-\cdot}$

0.031(N) 0.339(2H) 2.169(N) mT

14

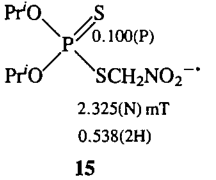

15

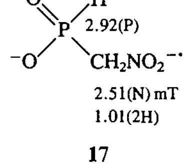

17

TABLE 4. Magnetic non-equivalence of β-protons in radicals of the type $XYZCCH_2NO_2^{-\bullet}$ [a]

			Hyperfine splittings/mT				ΔH/mT	
X	*Y*	*Z*	*a*(N)	*a*(β-H)	*a*(β-H')	*a*(γ-H)	(inner)	(outer)
H	Me	OH	2.51	1.12	0.97	0.06	0.04	0.025
H	Me	OEt	2.50	1.21	0.86	0.06	0.04	0.025
H	Me	OAc	2.47	1.27	0.68	0.06	0.04	0.03
H	Me	CO_2^-	2.51	1.44	0.68	0.06	0.03	0.02
H	$CH_2CO_2^-$	CO_2^-	2.51	1.22	0.94	0.06	0.055	0.02
H	Me	CO_2^-	2.47	1.34	0.66	0.06	0.04	0.025
H	CO_2^-	Cl	2.49	1.64	0.41	0.08	0.035	0.015

[a] Taken from ref. 24; $g = 2.0050$.

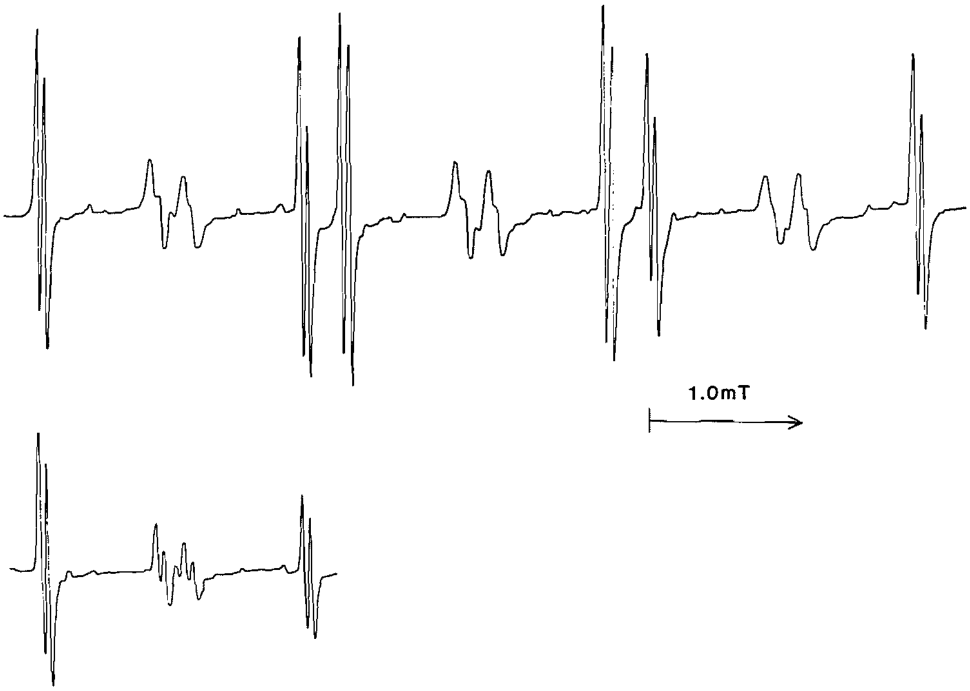

FIG. 4. An example of an adduct $XYZCCH_2NO_2^{-\bullet}$ with non-equivalent splittings from diastereotopic β-protons: $^-O_2CCH_2CH(CO_2^-)CH_2NO_2^{-\bullet}$ (from $SO_4^{-\bullet}$ and succinate) at 20°C, showing the marked line-broadening of the inner lines of the proton hyperfine pattern. The peaks inset are from the low-field components at 40°C.

These phenomena have been discussed in some detail elsewhere (24, 43) and the arguments will not be rehearsed here; however, it might simply be noted now that for these adducts and related nitroxides (43) (e.g. $XYZCCH_2N(Bu^t)O\cdot$) both the differences between the two non-equivalent splittings *and* the extent of differential line-broadening increase with the bulk of the γ-substituents (being particularly marked for carboxylate, chlorine and bromine substituents, see e.g. **18** (24)). This observation can in itself serve a useful diagnostic purpose, as in the characterization of $\cdot CHBrCO_2^-$ (not directly detectable) in the reaction of ·OH with bromoethanoate (see Fig. 5).

Kinetic and mechanistic studies of radical reactions

Finally, we illustrate with several examples how the knowledge of the structures of adducts $XCH_2NO_2^{-\bullet}$, as revealed by *a*(N), *a*(H), *g* etc., can prove helpful in mechanistic and kinetic studies; particular emphasis will be placed upon examples where

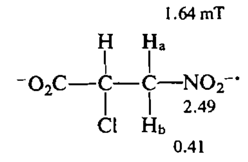

$$^-O_2C-CH(Cl)-CH_aH_b-NO_2^{-\bullet}$$

18

ΔH(inner) 0.035 mT
ΔH(outer) 0.015 mT

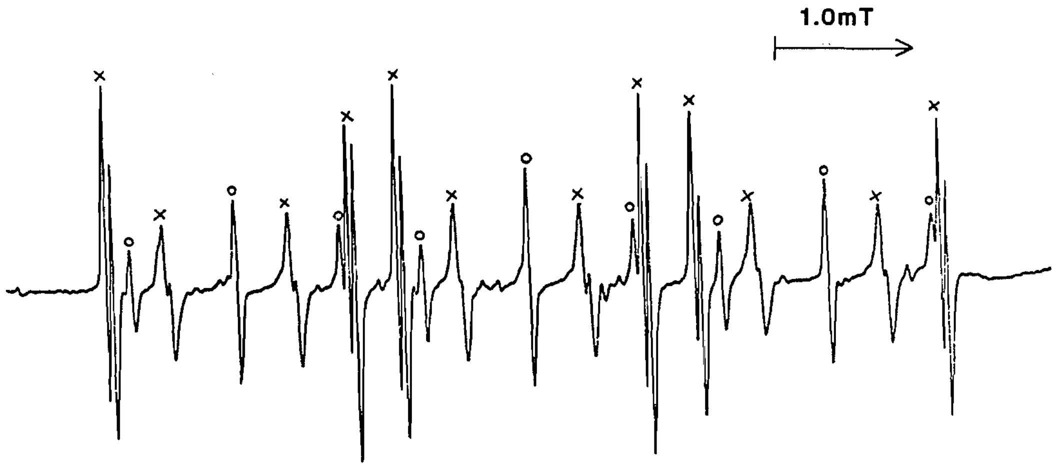

FIG. 5. Electron spin resonance spectrum of $BrCH(CO_2^-)CH_2NO_2^{-\bullet}$ (×) (with a(β-H) 1.60, 0.50 mT) formed in the reaction of ·OH with bromoethanoate in the presence of $CH_2{:}NO_2^-$; peaks marked O are from $HOCH_2NO_2^{-\bullet}$.

TABLE 5. Electron spin resonance spectra of radicals generated from alkoxy radicals in the presence of $CH_2NO_2^{-a}$

Alkoxy radical	$RCH_2NO_2^{-\bullet}$ R =	Hyperfine splitting/mT a(N)	a(β-H)	a(other)
$Bu^tO\cdot$	Bu^tO—	2.53	1.01(2H)	
	Me—	2.60	0.97(2H)	0.05(3H)
PrO·	PrO—	2.38	0.85(2H)	
	EtCH(OH)—	2.52	1.15(1H), 0.93(1H)	0.06(1H)
BuO·	BuO—	2.38	0.85(2H)	
	PrCH(OH)—	2.48	1.22(1H), 0.96(1H)	0.05(1H)
	$HOCH_2CH_2CH_2$—	2.51	1.03(2H)	0.05(2H)
$CH_2{=}CHCH_2CH_2CH_2O\cdot$	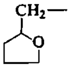	2.55	1.06(1H), 0.94(1H)	0.06(2H)
$MeCH_2CH_2CH_2CMe_2O\cdot$	$Me_2C(OH)CH_2CH_2CHMe$—	2.46	1.01(1H), 0.93(1H)	0.06(2H)
	$MeCH_2CH_2CH_2$—	2.46	1.00(2H)	0.06(2H)

[a] g = 2.0050.

the intermediate radicals themselves are not directly detectable in solution by esr (e.g. RO·, $RCO_2\cdot$) or where the radicals show particularly high reactivity, and hence a low, often undetectable, signal-to-noise ratio.

(a) Decomposition of alkyl hydroperoxides. It is found (14, 31) that when various alkyl hydroperoxides are reduced by Ti^{III} in a flow system in the presence of $CH_2{:}NO_2^-$, adducts formed from the appropriate alkoxyl radicals (RO·) can be detected (reactions [4] and [14]). Alkoxyl radicals are also

[4] $ROOH + Ti^{III} \rightarrow RO\cdot + OH^- + Ti^{IV}$

[14] $RO\cdot + CH_2NO_2^- \rightarrow ROCH_2NO_2^{-\bullet}$

[15] $HO\cdot + (RO)_2S{=}O \rightarrow RO\cdot + ROSO_2H$

[16] $RO\cdot \xrightarrow{-O} R'\cdot$

[17] $R'\cdot + CH_2NO_2^- \rightarrow R'CH_2NO_2^{-\bullet}$

formed in the reaction between HO· and dialkyl sulphites (reaction [15]), and they have been characterized similarly (44).[1]

In these reactions, the concentration of the spin trap employed is crucial; thus although at high concentrations of spin trap the corresponding alkoxyl radical can in many cases be intercepted, to give $ROCH_2NO_2^{-\bullet}$, other reactions of the alkoxyl radical (fragmentation, rearrangement) can compete effectively with the addition at lower values of $[CH_2NO_2^-]$, and secondary radicals (·R′) can be characterized (reactions [16] and [17]); parameters of the appropriate radicals are given in Table 5.

---

[1] Confirmation that alkoxy adducts have been correctly identified derives from the independent generation of the radical assigned the structure $EtOCHMeNO_2^{-\bullet}$ (from EtO· and $CHMe{:}NO_2^-$) from the reaction between ·CHMeOEt (from ·OH and diethyl ether) and NO_2^- (45).

For example, in experiments with $\mathrm{Bu^tO_2H}$ and $\mathrm{Ti^{III}}$, the methyl radical (see reactions [18] and [19]) is directly detectable (45). When the experiment is carried out in the presence of $\mathrm{CH_2{:}NO_2^-}$, the spectrum of $\mathrm{MeCH_2NO_2^{-\cdot}}$ becomes detectable; at pH 9.5, with $[\mathrm{CH_2{:}NO_2^-}]$ ca. 10^{-3} mol dm^{-3} the methyl radical is completely scavenged in this way (reaction [7]). Knowledge of the steady-state concentration of Me· in the absence of nitromethane (ca. 10^{-6} mol dm^3) and the rate constant for self-termination of ·Me (ca. 5×10^9 dm^{-3} mol^{-1} s^{-1} (46)) leads to the conclusion that to scavenge Me· in this way the rate constant for the addition reaction [7] must be $>10^7$ dm^3 mol^{-1} s^{-1}. When $[\mathrm{CH_2{:}NO_2^-}]$ is raised, the signal from $\mathrm{MeCH_2NO_2^{-\cdot}}$ is joined by that attributed to $\mathrm{Bu^tOCH_2NO_2^{-\cdot}}$ (with a 1:1 ratio of the Me· and $\mathrm{Bu^tO\cdot}$ adducts for $[\mathrm{CH_2{:}NO_2^-}]$ ca. 0.005 mol dm^{-3}): we conclude that addition now competes with fragmentation and also, employing steady-state analysis of the kind described in ref. (14), that k_{20}/k_{19} is ca. 2×10^2 dm^3 mol^{-1}.

[18] $\mathrm{Bu^tO_2H + Ti^{III} \rightarrow Ti^{IV} + OH^- + Bu^tO\cdot}$

[19] $\mathrm{Bu^tO\cdot \rightarrow Me_2C{=}O + Me\cdot}$

[7] $\mathrm{Me\cdot + CH_2{:}NO_2^- \rightarrow MeCH_2NO_2^{-\cdot}}$

[20] $\mathrm{Bu^tO\cdot + CH_2{:}NO_2^- \rightarrow Bu^tOCH_2NO_2^{-\cdot}}$

Other reactions which can be demonstrated (14) in this way include the 1,2-shift typical of primary alkoxy radicals in aqueous solution (reactions [21] and [22]) and the competing 1,5-shift in [23] (with $k_{22} \simeq k_{23}$); from experiments in which the 1,2-shift is in competition with intermolecular hydrogen-atom abstraction (e.g. the formation of $\mathrm{\cdot CH_2OH}$ from PrO· and $\mathrm{CH_3OH}$) it is suggested that the pseudo first-order rate constant k_{21} is ca. 10^7 s^{-1} (k_{22} and k_{23} are presumably also of this magnitude), and the lower limit for addition of propoxyl to $\mathrm{CH_2{:}NO_2^-}$ is estimated as 10^8 dm^3 mol^{-1} s^{-1}. It is likely that k_{20} is $>10^8$ dm^3 mol^{-1} s^{-1} (it may be as high as 10^9 dm^3 mol^{-1} s^{-1}) and that k_{19} is in the range 10^6–10^7 s^{-1} (much faster than the fragmentation rate in non-aqueous solution, cf. ref. 47). Particularly rapid reactions ($>10^8$ s^{-1}) are the cyclisation (reaction [24]) and the fragmentation and intramolecular abstraction reactions [25] and [26], in which no intermediate alkoxyl radicals could be intercepted.

[21] $\mathrm{CH_3CH_2CH_2{-}O\cdot \xrightarrow{(H_2O)} CH_3CH_2\dot{C}HOH}$

[22] $\mathrm{CH_3CH_2CH_2CH_2{-}O\cdot \rightarrow CH_3CH_2CH_2\dot{C}HOH}$

[23] $\mathrm{CH_3CH_2CH_2CH_2{-}O\cdot \rightarrow \cdot CH_2CH_2CH_2CH_2OH}$

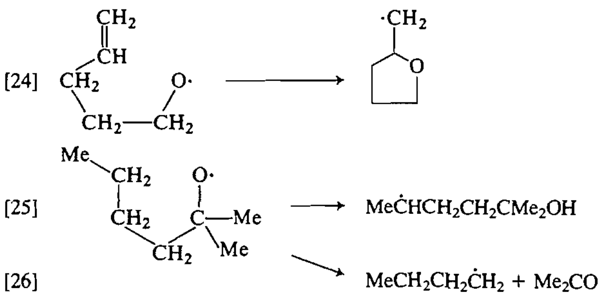

(b) Generation and reaction of aroyloxyl and acyloxyl radicals. As mentioned earlier, oxidation of benzoate ion with $\mathrm{SO_4^{-\cdot}}$ in the presence of $\mathrm{CH_2{:}NO_2^-}$ at pH 9 led to the detection of signals assigned to $\mathrm{PhCO_2CH_2NO_2^{-\cdot}}$ and $\mathrm{PhCH_2NO_2^{-\cdot}}$ (evidently formed as in reactions [9] and [10]), as well as to those of $\mathrm{O_2NCH_2CH_2NO_2^{-\cdot}}$ and $\mathrm{^-O_3OSCH_2NO_2^{-\cdot}}$ formed by direct reaction between $\mathrm{SO_4^{-\cdot}}$ and the trap (32). The assignment $\mathrm{PhCO_2CH_2NO_2^{-\cdot}}$ has been challenged (27, 48) on the grounds that an (unassigned) spectrum with these parameters is also detected from the reaction between photolytically generated $\mathrm{SO_4^{-\cdot}}$ and $\mathrm{CH_2{:}NO_2^-}$ in the absence of benzoate (48). However, important structural evidence (which also provides interesting mechanistic insight) that the assignments to $\mathrm{PhCO_2CH_2NO_2^{-\cdot}}$ (**10**) and $\mathrm{PhCH_2NO_2^{-\cdot}}$ (**11**) are correct stems from the observation that these same two signals are detected (32) when peroxybenzoic acid is reduced by $\mathrm{Ti^{III}}$ under identical conditions. As expected if reactions [27]–[30] are involved, the intensity of the signal assigned to **10** increased at the expense of **11** as $[\mathrm{CH_2{:}NO_2^-}]$ was increased (precisely as found for the $\mathrm{PhCO_2^-/SO_4^{-\cdot}}$ oxidation). An upper limit for the decarboxylation of benzoyloxyl of ca. 2.5×10^5 s^{-1} is calculated from the concentration of nitromethane needed to capture $\mathrm{PhCO_2\cdot}$ (35).

[27] $\mathrm{PhCO_2OH + Ti^{III} \rightarrow PhCO_2\cdot + OH^- + Ti^{IV}}$

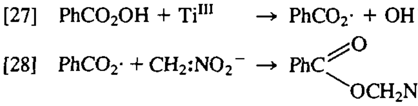

[28] $\mathrm{PhCO_2\cdot + CH_2{:}NO_2^- \rightarrow PhC({=}O)OCH_2NO_2^{-\cdot}}$

10

[29] $\mathrm{PhCO_2\cdot \rightarrow Ph\cdot + CO_2}$

[30] $\mathrm{Ph\cdot + CH_2{:}NO_2^- \rightarrow PhCH_2NO_2^{-\cdot}}$

11

For some substituted aromatic derivatives, however, oxidation of $\mathrm{ArCO_2^-}$ by $\mathrm{SO_4^{-\cdot}}$ and reduction of the corresponding peroxyacid by $\mathrm{Ti^{III}}$ led to contrasting esr observations. For example, *p*-peroxytoluic acid and $\mathrm{Ti^{III}}$ gave not only the adducts attributed the structures **19** and **20** but also a weak signal of the adduct **21**; in the oxidation of *p*-toluate with $\mathrm{SO_4^{-\cdot}}$, however, only **19** and **21**

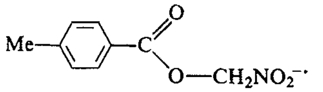

19

a(N)	2.39 mT
a(2H)	0.74 mT
g	2.0050

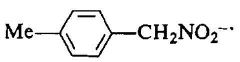

20

a(N)	2.565 mT
a(2H)	0.95 mT
g	2.0050

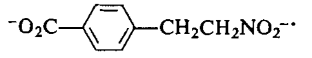

21

a(N)	2.55 mT
a(2H)	0.945 mT
a(2H)	0.076 mT
g	2.0050

could be detected, with no trace of **20**. Increase of $CH_2{:}NO_2^-$ in the former system led to an increase of [**19**] at the expense of [**20**] and [**21**], whereas in the latter experiment the ratio of [**19**] to [**21**] remained constant.

These results cannot be rationalized on the basis of a scheme in which a common intermediate ($MeC_6H_4CO_2\cdot$) is formed *directly* from both $ArCO_2^-$ and $ArCO_3H$ in the two systems. Our findings can, however, be rationalized by the mechanism outlined in Scheme 5; we envisage that in the peroxyacid reduction, the aroyloxyl radical (**22**), once formed, can undergo competing reactions involving fragmentation (to give the aryl radical, which is then trapped), addition to $CH_2{:}NO_2^-$, and intermolecular hydrogen abstraction from *p*-toluate formed *in situ* to give, ultimately **21** (the benzyl radical itself can be directly detected in the absence of trap; its signal is intensified when *p*-toluate is added to the system). In contrast, in the oxidation of *p*-toluate with $SO_4^{-\cdot}$ the relatively low concentration of aroyloxyl radical trapped and the much stronger signal from **21** — and the invariance of their ratio with [$CH_2NO_2^-$] — implies that a first-formed intermediate (evidently the radical-cation **23**, *cf.* also ref. 49) is partitioned between loss of a proton, to give the benzyl radical, and conversion into the aroyloxyl radical *before* trapping with $CH_2{:}NO_2^-$. Our finding thus emphasizes the fact that **22** and **23** are not representations (canonical forms) of a single species but that the two are distinct chemical entities; these results are in accord with the suggestion (50) that **22** is a σ-radical (*cf.* **24**), with the unpaired electron in an in-plane σ-orbital, in contrast with the structure of the π-type zwitterion **23** (*cf.* **25**) (examples of this type of radical have been characterized by esr (49)).

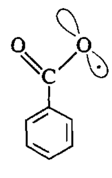

24

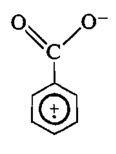

25

Similar observations were made for the reactions of *o*-toluate and *o*-peroxytoluic acid with the notable difference that in the reduction of the peracid in the presence of the trap a much greater concentration of the benzyl-type adduct was obtained; this is consistent with the occurrence of very rapid intramolecular hydrogen-atom transfer in the aroyloxyl radical (reaction [31]).

[31] 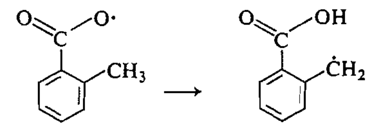

Decomposition with Ti^{III} of a variety of peroxoacids (formed in the perhydrolysis of esters and anhydrides with HO_2^- at ca. pH 9) is also thought to proceed via the corresponding aroyloxyl and acyloxyl radicals as precursors of decarboxylated radicals (Ar·, R·) (35). Although the acetoxyl radical was not itself trapped, some aliphatic acyloxy radicals $RCO_2\cdot$ (R = cyclopropyl, $CH_2{=}CH$) live

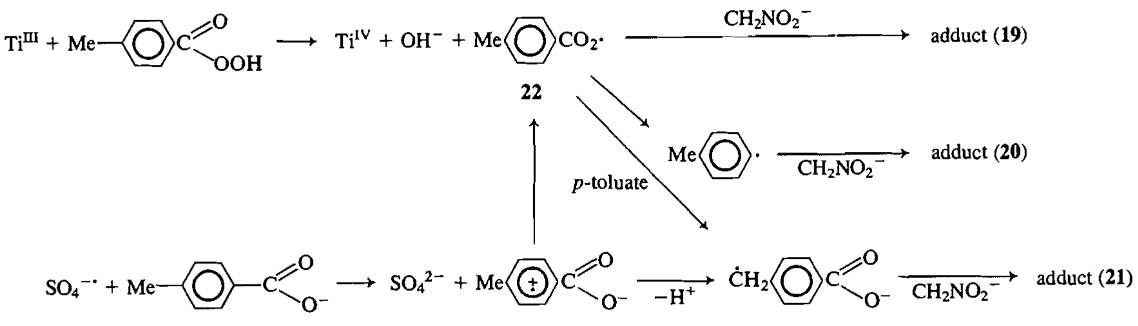

SCHEME 5

long enough to be detected via their adducts with the nitromethane *aci*-anion: the rate constants of their decarboxylation are thought to be in the range 10^5–10^7 s^{-1}.

Acknowledgements

We thank the S.R.C. for financial assistance for this work and the Royal Society of Chemistry for providing travel assistance (Career Award) for B.C.G.

1. (*a*) A. H. Maki and D. H. Geske. J. Am. Chem. Soc. **83**, 1852 (1961); (*b*) D. H. Geske, J. L. Ragle, M. A. Bambenek, and A. L. Balch. J. Am. Chem. Soc. **86**, 987 (1964).
2. P. Ludwig, T. Layloff, and R. N. Adams. J. Am. Chem. Soc. **86**, 4568 (1964).
3. R. L. Ward. J. Chem. Phys. **30**, 852 (1959); J. Am. Chem. Soc. **83**, 1296 (1961).
4. T. Fujinaga, Y. Deguchi, and K. Umemoto. Bull. Chem. Soc. Jpn. **37**, 822 (1964).
5. (*a*) G. A. Russell, E. G. Janzen, and E. T. Ström. J. Am. Chem. Soc. **86**, 1807 (1964); (*b*) R. C. Kerber, G. W. Urry, and N. Kornblum. J. Am. Chem. Soc. **87**, 4520 (1965).
6. A. K. Hofmann, A. M. Feldman, E. Gelblum, and W. G. Hodgson. J. Am. Chem. Soc. **86**, 639 (1964).
7. T. M. McKinney and D. H. Geske. J. Chem. Phys. **44**, 2277 (1966).
8. J. H. Freed and G. K. Fraenkel. J. Chem. Phys. **40**, 1815 (1964); **41**, 699 (1964).
9. W. M. Gulick, Jr. and D. H. Geske. J. Am. Chem. Soc. **87**, 4049 (1965); J. Gendell, J. H. Freed, and G. K. Fraenkel. J. Chem. Phys. **37**, 2832 (1962).
10. P. Neta and D. Meisel. J. Phys. Chem. **80**, 819 (1976).
11. P. B. Ayscough, A. J. Elliott, and G. A. Salmon. J. Chem. Soc. Faraday Trans. I, **74**, 511 (1978).
12. (*a*) B. C. Gilbert and M. Trenwith. J. Chem. Soc. Perkin Trans. II, 2010 (1973); (*b*) J. Spanget-Larsen. Theor. Chim. Acta, **51**, 65 (1979).
13. B. C. Gilbert, R. O. C. Norman, and P. S. Williams. J. Chem. Soc. Perkin Trans. II, 207 (1981).
14. B. C. Gilbert, R. G. G. Holmes, H. A. H. Laue, and R. O. C. Norman. J. Chem. Soc. Perkin Trans. II, 1047 (1976).
15. G. Czapski. J. Phys. Chem. **75**, 2957 (1971); B. C. Gilbert, R. O. C. Norman, and R. C. Sealy. J. Chem. Soc. Perkin Trans. II, 2174 (1973).
16. D. Behar and R. W. Fessenden. J. Phys. Chem. **76**, 1710 (1972).
17. M. McMillan and R. O. C. Norman. J. Chem. Soc. B, 590 (1968).
18. A. Albert and E. P. Serjeant. Ionization constants of acids and bases. Methuen, London. 1962.
19. D. J. Edge and R. O. C. Norman. J. Chem. Soc. B, 182 (1969).
20. K.-D. Asmus and I. A. Taub. J. Phys. Chem. **72**, 3382 (1968).
21. K.-D. Asmus, A. Henglein, and G. Beck. Ber. Busenges. Phys. Chem. **70**, 459 (1966).
22. M. C. R. Symons. J. Am. Chem. Soc. **91**, 5924 (1969).
23. B. C. Gilbert, R. O. C. Norman, G. Placucci, and R. C. Sealy. J. Chem. Soc. Perkin Trans. II, 885 (1975).
24. B. C. Gilbert, J. P. Larkin, and R. O. C. Norman. J. Chem. Soc. Perkin Trans. II, 1272 (1972).
25. D. J. Edge, R. O. C. Norman, and P. M. Storey. J. Chem. Soc. B, 1096 (1970).
26. D. J. Edge and R. O. C. Norman. J. Chem. Soc. B, 1083 (1970).
27. H. Zemel and R. W. Fessenden. J. Phys. Chem. **79**, 1419 (1975).
28. N. H. Anderson, M. McMillan, and R. O. C. Norman. J. Chem. Soc. B, 1075 (1970).
29. E. G. Janzen. Top. Stereochem. **6**, 177 (1971).
30. M. C. R. Symons and J. H. Sharp. Nature, **224**, 1297 (1969); C. Chachaty. C. R. Hebd. Seances Acad. Sci. **262**, 680 (1966); C. Chachaty and C. Rosilio. J. Chim. Phys. Phys. Chim. Biol. **64**, 777 (1967).
31. B. C. Gilbert, R. G. G. Holmes, and R. O. C. Norman. J. Chem. Res. (M) 0101, (S) 1 (1977).
32. B. Ashworth, B. C. Gilbert, R. G. G. Holmes, and R. O. C. Norman. J. Chem. Soc. Perkin Trans. II, 951 (1978).
33. N. H. Anderson and R. O. C. Norman. J. Chem. Soc. B, 993 (1971).
34. A. J. Dobbs, B. C. Gilbert, and R. O. C. Norman. J. Chem. Soc. Perkin Trans. II, 786 (1972).
35. B. C. Gilbert, R. G. G. Holmes, P. D. R. Marshall, and R. O. C. Norman. J. Chem. Res. (S) 172, (M) 1949 (1977).
36. R. O. C. Norman and P. M. Storey. J. Chem. Soc. B, 1009 (1971).
37. B. C. Gilbert, J. P. Larkin, and R. O. C. Norman. J. Chem. Soc. Perkin Trans. II, 272 (1973).
38. G. Brunton, B. C. Gilbert, and R. J. Mawby. J. Chem. Soc. Perkin Trans. II, 650 (1976).
39. B. C. Gilbert, J. P. Larkin, R. O. C. Norman, and P. M. Storey. J. Chem. Soc. Perkin Trans. II, 1508 (1972).
40. A. L. J. Beckwith. Aust. J. Chem. **25**, 1887 (1972).
41. P. J. Krusic and J. K. Kochi. J. Am. Chem. Soc. **93**, 846 (1971).
42. J. A. Howard, Y. Ohkatsu, J. H. B. Chenier, and K. U. Ingold. Can. J. Chem. **51**, 1543 (1973).
43. B. C. Gilbert and M. Trenwith. J. Chem. Soc. Perkin Trans. II, 1834 (1973).
44. B. C. Gilbert, H. A. H. Laue, R. O. C. Norman, and R. C. Sealy. J. Chem. Soc. Perkin Trans. II, 1040 (1976).
45. M. F. R. Mulcahy, J. R. Steven, and J. C. Ward. Aust. J. Chem. **18**, 1177 (1965).
46. B. C. Gilbert, R. O. C. Norman, and R. C. Sealy. J. Chem. Soc. Perkin Trans. II, 303 (1975).
47. D. J. Carlsson and K. U. Ingold. J. Am. Chem. Soc. **89**, 4891 (1967).
48. H. Zemel and R. W. Fessenden. J. Phys. Chem. **82**, 2670 (1978).
49. S. Steenken, P. O'Neill, and D. Schulte-Frohlinde. J. Phys. Chem. **81**, 26 (1977).
50. M. B. Yim, O. Kikuchi, and D. E. Wood. J. Am. Chem. Soc. **100**, 1869 (1978); J. M. McBride and R. A. Merrill. J. Am. Chem. Soc. **102**, 1723 (1980).